Orbital
The electronic journal of chemistry

the electronic journal of chemistry

Full Paper | http://dx.doi.org/10.17807/orbital.v14i2.15596

# Hydrogenation of Biomass-derived 5-Hydroxymethylfurfural (HMF) over Pd Catalysts in Aqueous Medium

Wesley Romário da Silva, José Maurício Rosolen, and Paulo Marcos Donate

We hydrogenated biomass-derived 5-hydroxymethylfurfural (HMF) in aqueous medium in a reaction catalyzed by palladium nanoparticles (Pd) on carbonaceous materials with different morphology and hydrophobic degree. The Pd catalysts were prepared by dipping the carbonaceous material into a $Pd^0$ micro-emulsion. The catalyst support affected catalytic HMF hydrogenation. By using micrometric active carbon (AC) combined with cup-stacked carbon nanotubes (CSCNTs) and Pd, we obtained a micro/nanostructured material designated Pd/CSCNT-AC, which performed better than the other carbonaceous materials containing similar Pd loading. Pd/CSCNT-AC catalyzed HMF hydrogenation at the C=O double bond more selectively, giving between 85% and 99% selectivity toward 2,5-bis(hydroxymethyl)furan (BHMF). We also investigated how temperature, hydrogen pressure, and reaction time affected HMF hydrogenation.

## Graphical abstract

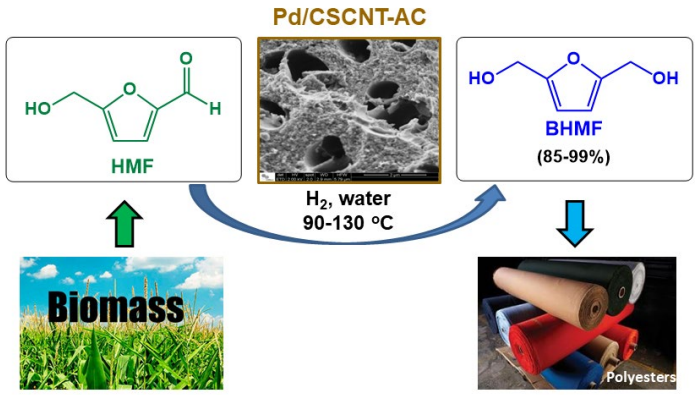


## Keywords

Aqueous medium hydrogenation
carbon nanotube/charcoal composite
HMF
5-hydroxymethylfurfural
Palladium nanoparticles

## Article history

**Received** 22 Apr 2022
**Revised** 17 Jun 2022
**Accepted** 17 Jun 2022
**Available online** 02 Jul 2022

**Handling Editor:** Adilson Beatriz

## 1. Introduction

The renewable nature of lignocellulosic biomass and its potential conversion into value-added products have attracted researchers' attention over the past years [1-4]. Among biomass-derived products, 5-hydroxymethylfurfural (HMF) is a key intermediate because it displays various types of chemical functions and is easy to obtain from carbohydrates [5-7]. Moreover, HMF is a potential starting material to prepare bio-based chemicals, such as biopolymers and liquid biofuels, and to synthesize chemical derivatives of high commercial value [8, 9]. In this context, HMF hydrogenation yields building blocks that could replace petrochemicals in numerous applications [9-13]. However, selective HMF transformation into the desired product is challenging. For example, HMF hydrogenation generally produces a mixture of hydrogenated products in both the side chain and furan ring, together with ring-opening products [5, 12, 13]. In the presence of the

Department of Chemistry, Faculdade de Filosofia, Ciências e Letras, Universidade de São Paulo, Avenida Bandeirantes 3900, zip code 14040-901, Ribeirão Preto, São Paulo, Brazil. *Corresponding author. E-mail: **pmdonate@usp.br**

traditional commercial catalyst 5% Pd/C, HMF hydrogenation occurs through three types of reactions: decarbonylation to furfuryl derivatives, conversion to dimethylfuran, and hydrogenation/hydrogenolysis to tetrahydrofurans [14]. Another issue about HMF transformation is that the reactions require large amounts of solvents, which has raised environmental concerns. In most published works, HMF hydrogenation involves the use of organic solvents, some of which are toxic, expensive, and non-renewable (e.g., ionic liquids, tetrahydrofuran, 1,4-dioxane, and alcohols). From a green chemistry viewpoint, performing catalytic reactions in water is more attractive [15]. In addition, HMF reactions carried out in water are much more practical because HMF is usually directly supplied in aqueous solutions, minimizing costs and dismissing the need for purification steps [12].

HMF hydrogenation in the presence of heterogeneous catalysts has been widely studied due to its advantages, including its easy separation from the reaction medium and possible recycling. The most largely adopted heterogeneous catalysts are represented by metals, such as Ru, Pt, Pd, Au, Ir, Ni, and Cu, supported on several oxides, polymers, or carbon species [12,13]. In acidic solution, the major products of HMF hydrogenation are 1,2,5,6-hexanetetrol, 1-hydroxyhexane-2,5-dione and 1,2,5-hexanetriol [5], as outlined in Scheme 1.

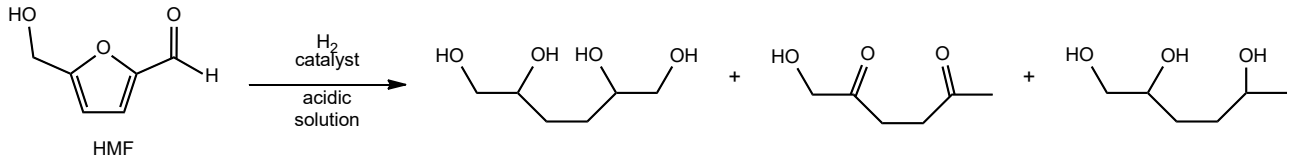


**Scheme 1.** Catalytic HMF hydrogenation in acidic solution.

As outlined in Scheme 2, HMF conversion to BHMF [2,5-bis(hydroxymethyl)furan] via selective C=O hydrogenation or to BHMTHF [2,5-bis(hydroxymethyl)tetrahydrofuran] via further C=C furan ring hydrogenation can be highly selective (80–100%) when heterogeneous catalysts are employed in organic medium or neutral solution [5,12,13,16-20]. A comparison of several catalytic systems, including the role played by the catalytic nanoparticles at the molecular level and the experimental conditions, has been published for HMF hydrogenation [18-24].

HMF hydrogenation in aqueous medium can afford different products — this reaction environment can promote hydrolytic furan ring opening, hydrodeoxygenation, and furan ring rearrangements [12]. Therefore, HMF hydrogenation selectivity in aqueous medium to produce BHMF, HMTHF [5-(hydroxymethyl)tetrahydrofurfural], or BHMTHF, or a combination of these products, is markedly determined by the hydrogenation activity and other properties of the chosen catalytic system. For HMF hydrogenation in water, functional sites in a catalytic reaction system based on supported metal catalysts determine product selectivity. Nevertheless, the role that the carbon support plays in heterogeneous catalysts in the presence of water as solvent is unclear. Additionally, the field of green chemistry lacks comparative studies about catalysts containing hydrophilic or hydrophobic surfaces with different morphology.

For this reason, we have decided to investigate HMF hydrogenation catalyzed by palladium nanoparticles (Pd) supported on three distinct micrometric carbonaceous substrates. The first substrate was natural micrometric hydrophobic spheroid graphite (G) consisting of crumpled graphite basal planes that form a potato that is difficult to wet, but which is relatively denser than graphite crystals floating in aqueous medium [25]. The second substrate was commercial activated carbon resulting from eucalyptus pyrolysis followed by activation (AC), which can adsorb water in its pores [26]. The third substrate was a micro/nanostructured composite consisting of AC whose surface is covered with entangled carbon nanotubes whose walls contain cup-stacked carbon nanotubes (CSCNTs) with the extremity vertically attached to the AC surface [27-30]. CSCNTs can be prepared under specific CNT growth conditions and are not a commercial structure such as SWCNTs or MWCNTs. CSCNTs consist of diagonally stacked graphene walls and a hollow central conic channel, so their walls should be rich in dangling bonds that can favor chemical species adsorption [29,31]. However, more recently, CSCNTs have been shown to present special wettability properties even under high-vacuum conditions [32]. In fact, unlike hydrophobic MWCNTs, CSCNTs on the surface of hydrophobic carbonaceous materials have been reported to make the resulting composite hydrophilic [30]. So far, the use of CSCNT-AC has been little investigated in the field of catalysis or not investigated at all in the presence of water even though CSCNT-AC with different surfaces, shapes, and hydrophobic and/or hydrophilic sites can be synthesized, and its micro/nanostructure seems to diminish the environmental impact of nanostructures that contain CNTs [33-36]. Furthermore, CSCNT-AC does not demand CSCNT functionalization for dispersion in aqueous medium to be achieved. Therefore, we have evaluated whether Pd/CSCNT-AC is a selective catalyst for HMF hydrogenation in aqueous medium

## 2. Results and Discussion

### 2.1 CSCNT-AC and Pd catalyst composite characterization

This type of catalyst has already been characterized by our research group [35,37]. Below we briefly describe its main characteristics.

We prepared the Pd/CSCNT-AC composites by dipping the support into the Pd microemulsion. Transmission electron microscopy (TEM) analyses confirmed that Pd smaller than 5 nm adsorbed onto the external walls of the CSCNTs, whose diameter ranged from 30 to 80 nm. The TEM pictures also showed that the CSCNT walls did not have the typical CSCNT pattern. The cup-stacked, fish bone, or defective tubes presented a lot of dangling bonds on their surface, which could favor Pd dispersion. Indeed, Pd was well dispersed along the individual CSCNTs.

Figure 1 shows the scanning electron microscopy (SEM) pictures of typical, Pd/CSCNT-AC (Pd 2.0 wt%), Pd/AC (Pd 1.7 wt%), and Pd/G (Pd 2.2 wt%) grains. Pd/CSCNT-AC (Figure 1A and 1B) displayed a dense network of entangled CSCNTs covering the entire AC particle surface, but several cavities or nanometric pores were also evident. There was no CSCNT coating inside the large AC cavities (Figure 1B). The CSCNTs had different diameter, length, and curvature. Thus, the AC

substrate shape and surface porosity influenced the architecture of the resulting CSCNT coating network. In addition, detailed SEM analyses demonstrated that all the samples presented Pd clusters, which probably originated during the filtration procedure conducted after Pd was incorporated into the G, AC, or CSCNT-AC support. In the case of AC (Figure 1C) and G (Figure 1D), besides Pd nanoparticle agglomeration, the AC and G surface contained Pd nanoparticles dispersed across the whole surface. G presented several crystals stacked on top of each other. The edge of the graphite crystals concentrated most of the Pd clusters (inset Figure 1D). On the other hand, AC contained randomly formed Pd clusters (Figure 1C).

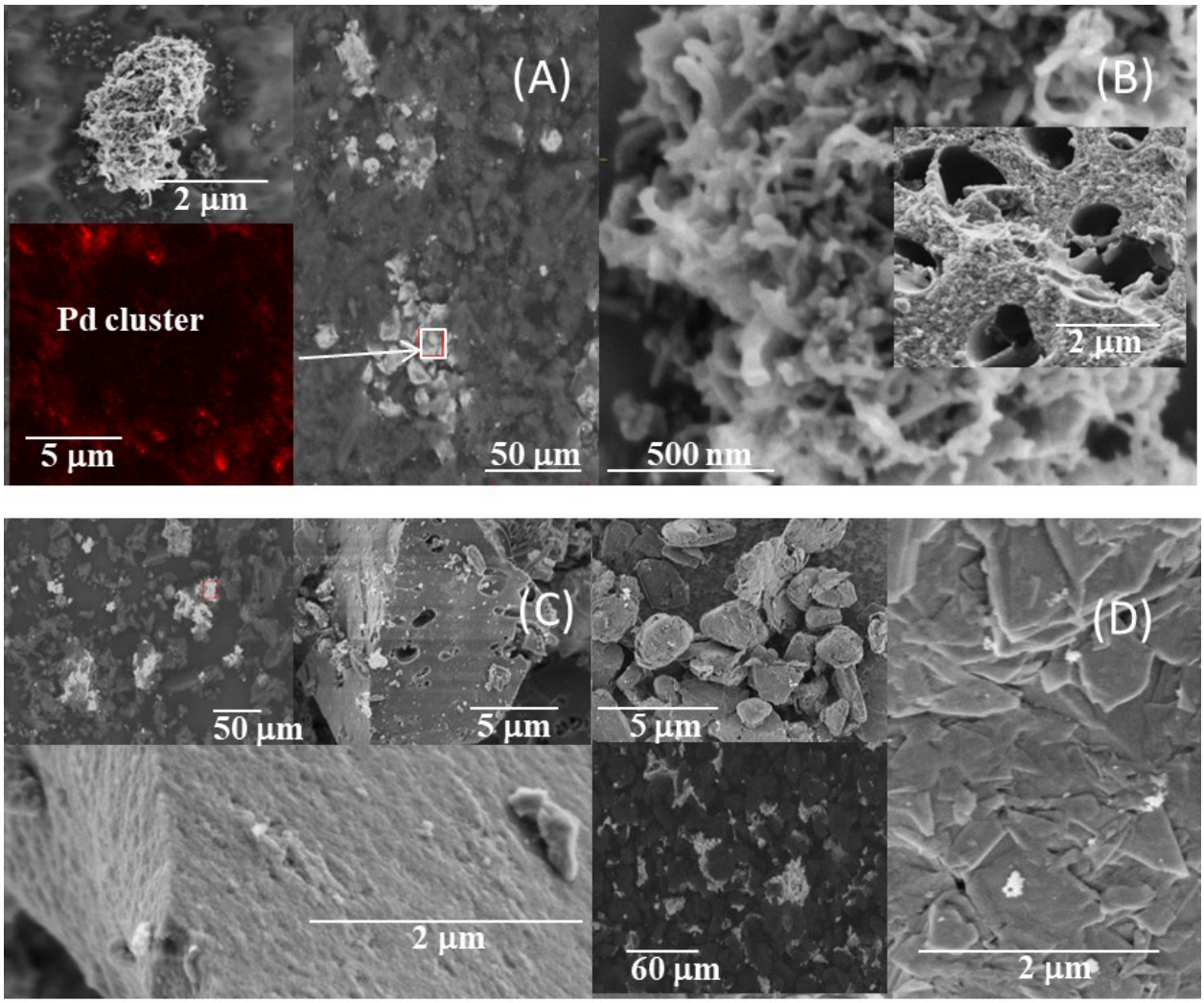


**Fig. 1.** SEM pictures of Pd/CSCNT-AC (**A**, **B**), Pd/AC (**C**), and Pd/G (**D**) at different magnifications. Pd nanoparticle agglomeration appears as bright points.

### 2.2 HMF hydrogenation

We investigated the Pd/G, Pd/AC, and Pd/CSCNT-AC catalytic activity and selectivity during HMF C=O and C=C double bond hydrogenation in aqueous medium, which could yield BHMF, HMTHF, and BHMTHF, as outlined in Scheme 2.

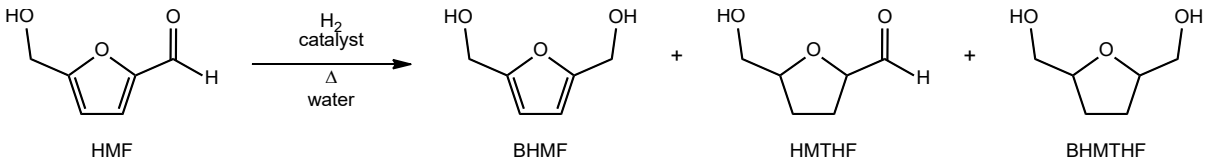


**Scheme 2.** Catalytic HMF hydrogenation.

First, we tested G, AC, and CSCNT-AC without Pd during HMF hydrogenation at high temperature and hydrogen pressure (130 °C and 4.8 MPa of $H_2$), but we did not detect any HMF conversion, even after reaction for 5 h. Next, we studied the reactions under different temperature (90 to 130 °C), hydrogen pressure (3.4 to 4.8 MPa), and reaction time (1, 2, and 3 h) conditions [37].

#### 2.2.1 Temperature effect on HMF hydrogenation

To examine how the reaction temperature affected HMF

hydrogenation, we tested Pd/G, Pd/AC, and Pd/CSCNT-AC at 90, 110, and 130 °C, at a constant hydrogen pressure of 3.4 MPa. Table 1 lists the results.

**Table 1.** Reaction temperature effect on HMF hydrogenation in aqueous medium after 2h.[a]

| Catalyst | Temperature (°C) | | | | | | | | |
|---|---|---|---|---|---|---|---|---|---|
| | 90 | | | 110 | | | 130 | | |
| | Conv. | $S_{BHMF}$ | $S_{HMTHF}$ | Conv. | $S_{BHMF}$ | $S_{HMTHF}$ | Conv. | $S_{BHMF}$ | $S_{HMTHF}$ |
| 0.7% Pd/G | <1% | - | - | <1% | - | - | 4% | >99% | - |
| 2.2% Pd/G | 15% | >99% | - | 17% | >99% | - | 31% | 32% | 68% |
| 1.0% Pd/AC | 5% | >99% | - | 6% | >99% | - | 10% | 80% | 20% |
| 1.7% Pd/AC | 20% | 75% | 25% | 22% | 23% | 23% | 36%[b] | - | - |
| 0.9% Pd/CSCNT-AC | 16% | >99% | - | 39% | >99% | - | 40% | >99% | - |
| 2.0% Pd/CSCNT-AC | 70% | 85% | 15% | 75% | 85% | 11% | 76% | 87% | 4% |

HMF conversion (**Conv.**) and selectivity (**S**) toward 2,5-bis(hydroxymethyl)furan (BHMF) and 5-(hydroxymethyl)-tetrahydrofurfural (HMTHF).
[a] Reaction conditions: 50 mg of HMF, 5 mg of catalyst, 6 mL of deionized water, 3.4 MPa of $H_2$, 2 h.
[b] A large quantity of by-products were formed.

Pd/G was less active than the other Pd catalysts with similar Pd concentration — 0.7% Pd/G exhibited low activity even at 130 °C (HMF conversion ~ 4%); 2.2% Pd/G was a little more active (HMF conversion ~ 15-31%). However, this small increase in activity decreased catalyst selectivity for BHMF formation at 130 °C.

Pd/AC was not very active, either. The maximum HMF conversion rate was 36% even at the highest temperature (130 °C). Pd/AC also displayed low selectivity. For example, 1.7% Pd/AC at 110 °C exhibited a selectivity of only 23% toward BHMF and HMTHF, and other by-products emerged. Compared to 2.2% Pd/G and 2.0% Pd/CSCNT-AC, which had similar Pd concentration, 1.7% Pd/AC had intermediate catalytic activity, but it generated a large quantity of by-products at 130 °C. We did not identify BHMF or HMTHF as reaction products when we used 1.7% Pd/AC as catalyst, but we detected considerable amounts of polymerization products and hydrogenolysis products, particularly 2,5-dimethylfuran and 2,5-dimethyltetrahydrofuran (both <1%). On the other hand, hydrophilic 1.0% Pd/AC exhibited low HMF conversion rate (<10%) even with rising temperature. Nevertheless, 1.0% Pd/AC selectivity toward BHMF dropped from >99% to 80% when we raised the temperature to 130 °C.

Pd/CSCNT-AC afforded the highest catalytic activity under the employed reaction conditions. The selectivity of >99% toward BHMF achieved with 0.9% Pd/CSCNT-AC at all temperatures indicated that this material was the most selective during HMF hydrogenation. In turn, 2.0% Pd/CSCNT-AC was the most active catalyst, with HMF conversion rates ranging from 70 to 76% at different reaction temperatures. On the other hand, at all the employed temperatures, 2.0% Pd/CSCNT-AC selectivity toward BHMF decreased to 85–87%. The higher Pd/CSCNT-AC catalytic activity toward selective HMF carbonyl hydrogenation was due to the high $Pd^0$ concentration. In addition, the CSCNT graphene electrons extended to Pd, which increased the metal charge density and made reactant adsorption through the C=C double bonds more difficult, thereby shifting selectivity toward C=O double bond hydrogenation [38].

### 2.2.2 Hydrogen pressure effect on HMF hydrogenation

To examine the hydrogen pressure effect on HMF hydrogenation, we tested Pd/G, Pd/AC, and Pd/CSCNT-AC under hydrogen pressure varying from 3.4 to 4.8 MPa, at constant temperature (110 °C). Table 2 compiles the results.

**Table 2.** Hydrogen pressure effect on HMF hydrogenation in aqueous medium after 2h.[a]

| Catalyst | $H_2$ pressure (MPa) | | | | | | | | |
|---|---|---|---|---|---|---|---|---|---|
| | 3.4 | | | 4.1 | | | 4.8 | | |
| | Conv. | $S_{BHMF}$ | $S_{HMTHF}$ | Conv. | $S_{BHMF}$ | $S_{HMTHF}$ | Conv. | $S_{BHMF}$ | $S_{HMTHF}$ |
| 0.7% Pd/G | <1% | - | - | 8% | >99% | - | 14% | 36% | 64% |
| 2.2% Pd/G | 17% | >99% | - | 73% | 82% | 10% | >99% | 48% | 6% |
| 1.0% Pd/AC | 6% | >99% | - | 37% | 59% | 38% | 46% | 58% | 33% |
| 1.7% Pd/AC | 22% | 23% | 23% | 44% | 3% | 24% | 67% | - | 33% |
| 0.9% Pd/CSCNT-AC | 38% | >99% | - | 38% | 92% | 8% | 39% | 89% | 11% |
| 2.0% Pd/CSCNT-AC | 75% | 85% | 11% | 78% | 77% | 23% | >99% | 76% | 24% |

HMF conversion (**Conv.**) and selectivity (**S**) toward 2,5-bis(hydroxymethyl)furan (BHMF) and 5-(hydroxymethyl)-tetrahydrofurfural (HMTHF).
[a] Reaction conditions: 50 mg of HMF, 5 mg of catalyst, 6 mL of deionized water, 110 °C, 2 h.

0.7% Pd/G showed low catalytic activity even under the highest hydrogen pressure. Concerning 2.2% Pd/G, an increase in hydrogen pressure from 3.4 to 4.8 MPa enhanced HMF conversion from 17% to >99% (Table 2). However, selectivity toward BHMF decreased from >99% to 48%, and by-products other than HMTHF arose.

Regarding 1.0% Pd/AC, higher hydrogen pressure augmented HMF conversion from 6% to 46%. However, by-product formation also increased, consequently reducing 1.0% Pd/AC selectivity toward BHMF from 99% to 58% (Table 2). In contrast, Pd/AC achieved maximum HMF conversion (67%) under 4.8 MPa of $H_2$. Selectivity toward HMTHF was only 33%, but no BHMF emerged. These results suggested that higher hydrogen pressure mitigated the hydrophobic phase influence on the reaction.

On the other hand, hydrophobic/hydrophilic Pd/CSCNT-AC was less sensitive to hydrogen pressure. An increase in hydrogen pressure from 3.4 to 4.8 MPa practically did not affect HMF conversion in the case of 0.9% Pd/CSCNT-AC (~38%). However, selectivity toward BHMF decreased from >99% under 3.4 MPa of $H_2$ to 89% under 4.8 MPa of $H_2$. As for 2.0% Pd/CSCNT-AC, an increase in hydrogen pressure from 3.4 to 4.8 MPa enhanced HMF conversion from 75% to >99% (Table 2). Again, increased hydrogen pressure reduced selectivity toward BHMF from 85% to 76% and favored HMTHF formation, which rose from 11% to 24%.

Generally, mild reaction conditions (0.1–1.0 MPa of $H_2$ and 15–60 °C) are required to limit the reaction toward BHMF formation from HMF. Higher reaction pressures (6–8 MPa of $H_2$) lead to total HMF hydrogenation to BHMTHF [19]. To our knowledge, the best catalytic performance for BHMF synthesis from HMF has been obtained with a $Cu/MgAlO_x$ catalyst, which produced BHMF in 92.7% yield at 100% conversion at 180 °C and 1.0 MPa of $H_2$ after reaction for 5 h in 1,4-dioxane [18-20]. The solvent nature affected product distribution. In fact, 1,4-dioxane and water favored BHMF formation, whereas 1-propanol and 2-propanol shifted the reaction to hydrogenolysis and etherification products. Besides, competitive adsorption on the active sites between solvents and HMF might decrease HMF conversion [20].

### 2.2.3 Reaction time effect on HMF hydrogenation

To verify how the reaction time affected HMF hydrogenation, we carried out reactions at 110 °C and hydrogen pressure of 3.4 MPa for different times. Table 3 summarizes the results.

**Table 3.** Reaction time effect on HMF hydrogenation in aqueous medium at 110 °C.[a]

| Catalyst | Reaction time (h) | | | | | | | | |
|---|---|---|---|---|---|---|---|---|---|
| | 1 | | | 2 | | | 3 | | |
| | Conv. | $S_{BHMF}$ | $S_{HMTHF}$ | Conv. | $S_{BHMF}$ | $S_{HMTHF}$ | Conv. | $S_{BHMF}$ | $S_{HMTHF}$ |
| 0.7% Pd/G | <1% | - | - | <1% | - | - | <1% | - | - |
| 2.2% Pd/G | 4% | >99% | - | 17% | >99% | - | 34% | 18% | 38% |
| 1.0% Pd/AC | 2% | >99% | - | 6% | >99% | - | 16% | - | 57% |
| 1.7% Pd/AC | 12% | 50% | 50% | 22% | 23% | 23% | 53% | - | 21% |
| 0.9% Pd/CSCNT-AC | 8% | >99% | - | 39% | >99% | - | 39% | 77% | 2% |
| 2.0% Pd/CSCNT-AC | 52% | 86% | 14% | 75% | 85% | 11% | 76% | 60% | 10% |

HMF conversion (**Conv.**) and selectivity (**S**) toward 2,5-bis(hydroxymethyl)furan (BHMF) and 5-(hydroxymethyl)-tetrahydrofurfural (HMTHF).

[a] Reaction conditions: 50 mg of HMF, 5 mg of catalyst, 6 mL of deionized water, 3.4 MPa of $H_2$, 110°C.

0.7% Pd/G was completely inactive under the tested conditions. In turn, 2.2% Pd/G yielded small HMF conversion (maximum of 34% after 3 h), but it was highly selective toward BHMF (>99% within 2 h of reaction). However, after reaction for 3 h, BHMF selectivity decreased from >99% to 18%, and by-products other than HMTHF were favored.

1.0% Pd/AC behaved similarly: HMF conversion was low (maximum of 16% after 3 h); selectivity toward BHMF was high (>99% within 2 h of reaction). Nevertheless, within only one extra hour, BHMF was totally consumed, producing 57% of HMTHF and other by-products. 1.7% Pd/AC provided maximum HMF conversion of 53% after 3 h, but selectivity toward both BHMF and HMTHF was low (Table 3).

Pd/CSCNT-AC afforded the best results: HMF conversion and selectivity toward BHMF formation were higher as compared to the catalysts discussed above (Table 3). Although 0.9% Pd/CSCNT-AC provided small HMF conversion (maximum of 39% after 2 h), selectivity toward BHMF was very high (>99% in up to 2 h of reaction), but it decreased a little (from >99% to 77%) after reaction for 3 h, producing small amounts of HMTHF (2%) and other by-products. 2.0% Pd/CSCNT-AC led to high HMF conversion, which increased from 52% after reaction for 1 h to 75% after reaction for 2 h and remained practically constant (76%) thereafter. This catalyst presented 86% and 14% selectivity toward BHMF and HMTHF, respectively, within only 1 h of reaction. After 2 h, selectivity dropped a little: 85% of BHMF, 11% of HMTHF, and about 4% of by-products. After reaction for 3 h, selectivity toward BHMF decreased to 60%, and 10% HMTHF and more by-products emerged (30%).

These results showed that long reaction times diminished Pd/CSCNT-AC selectivity. This probably happened because the initially formed BHMF underwent further hydrogenation or hydrogenolysis between 2 and 3 h, generating other by-products that negatively affected the catalyst. Indeed, the presence of BHMTHF was not detected.

### 2.2.4 Recycling experiment

We investigated 2% Pd/CSCNT-AC stability after several recycling HMF hydrogenation experiments at 110 °C and hydrogen pressure of 3.4 MPa for 2 h. After each reaction, the catalyst was recovered by filtration and washed with deionized water. Then, the recovered catalyst was reduced

under hydrogen pressure at 110 °C before the following cycle was initiated. As indicated in Table 4, the recycled catalyst exhibited consistent performance over five cycles.

**Table 4.** Effect of catalyst recycling on HMF hydrogenation catalyzed by 2% Pd/CSCNT-AC in aqueous medium at 110 °C.[a]

| Reaction | HMF Conversion | BHMF | HMTHF | Other by-products |
|---|---|---|---|---|
| 1 | 75% | 85% | 11% | 4% |
| 2 | 76% | 84% | 10% | 6% |
| 3 | 74% | 85% | 10% | 5% |
| 4 | 75% | 84% | 11% | 5% |
| 5 | 73% | 83% | 11% | 6% |

[a] Reaction conditions: 50 mg of HMF, 5 mg of catalyst, 6 mL of deionized water, 3.4 MPa of $H_2$, 110°C, 2h.

Compared to the fresh catalyst, the recycled catalyst exhibited good stability for HMF hydrogenation under the assessed conditions and was recycled at least five times without the catalytic activity dropping significantly. 2% Pd/CSCNT-AC also had satisfactory selectivity: selectivity did not vary significantly on going from one catalytic cycle to the next, and 83–85% and 10–11% BHMF and HMTHF were formed, respectively, in addition to 4–6% of other by-products (Table 4).

## 3. Material and Methods

### 3.1 Experimental details

5-Hydroxymethylfurfural (HMF), *n*-heptane, $NaBH_4$, and $PdCl_2$ were purchased from Sigma-Aldrich. Ethyl acetate was acquired from Tedia, and the surfactant Brij® 30 was obtained from Across Organics. Activated carbon (AC) (particle size = 325 mesh) and spheroid graphite (G) were purchased from Alpha Carbo Industrial.

The metal content in Pd/G, Pd/AC, and Pd/CSCNT-AC was determined by atomic absorption spectroscopy on a ContrAA 700 (Analytik Jena AG, Jena, Germany) apparatus [39]. To this end, approximately 20 mg of the catalyst (Pd/G, Pd/AC, or Pd/CSCNT-AC) was digested with 5 mL of concentrated HCl for 30 min. Then, the solution was filtered through a filter paper and diluted to 10.00 mL in a volumetric flask. The Pd dispersion on CSCNTs extracted from the Pd/CSCNT-AC surface was characterized by scanning electron microscopy (SEM) and transmission electron microscopy (TEM). SEM analyses were performed on a FEI-Quanta 650 FEG and FEI Inspect F50 microscopes, and TEM analyses were conducted on a JEOL JEM-100cx 485 microscope. The TEM grids were prepared with CSCNTs (mechanically removed from Pd/CSCNT-AC) dispersed in isopropyl alcohol and added dropwise onto lacey-carbon/copper grids (300 mesh). The X-ray Photoemission Spectroscopy (XPS) experiment was carried out with an Al K-α X-ray source in an ultra-high vacuum chamber ($10^{-9}$ torr). Mn 2p was recorded with energy resolution of 0.1 eV, dwell time of 1.0 s, and Constant Analyzer Energy (CAE) of 100 eV [37].

The starting material conversion rate and the product ratio after the hydrogenation reactions were determined on a gas chromatograph (GC-2010 Plus, Shimadzu Corporation) equipped with an FID detector and a Restek Rtx-5® fused silica capillary column (30-m length x 0.25- mm i.d.; 0.25-μm film thickness) operating at temperatures ranging from 40 to 280 °C. Products were identified by comparison with standard samples and analyzed on a Shimadzu GC/MS QP-2010 spectrometer operating with electron-impact ionization (EI, 70eV).

### 3.2 Composite preparation

The disordered CSCNT-AC composite substrate was prepared by using the same type of Chemical Vapor Deposition (CVD) reactor and growth parameters described by Matsubara *et al*. [27]. CSCNT-AC was prepared by growing the CNT network on the substrate (AC) by methanol CVD decomposition in the presence of Mn/Co catalyst, which provided tubes with a high concentration of defects. CNTs were grown at 650 °C, and nitrogen was employed as inert gas to feed the reaction with methanol vapor. The CSCNT concentration in the AC was 30 wt%; the Mn/Co catalyst concentration was ~10 wt%. Before Pd was incorporated into CSCNT-AC, the substrate was washed with concentrated HCl, which was followed by successive washings with deionized water. This procedure was applied to extract any Mn/Co nanoparticles that could be covering the graphene layers on the CSCNT tips.

### 3.3 Pd catalyst preparation

Metallic Pd was incorporated into G, AC, or CSCNT-AC by reverse microemulsion of water in organic phase and surfactant (Brij® 30). First, the microemulsions were prepared by adding a 0.10 mol $L^{-1}$ aqueous solution (5.2 g) of the metal precursor ($PdCl_2$ in 0.1 mol $L^{-1}$ HCl) to a mixture of *n*-heptane (28.3 g) and Brij® 30 (10.0 g) under stirring at 40 °C. The overall microemulsion composition was 12 wt% $H_2O$, 23 wt% Brij® 30 or polyethyleneglycol-dodecylether, and 65 wt% *n*-heptane. The Pd salt was reduced by rapidly adding a 2.00 mol $L^{-1}$ $NaBH_4$ aqueous solution (5.2 g) to the emulsion, and the mixture was kept under stirring at 40 °C for 30 min. This procedure yielded a black $Pd^0$ microemulsion [35]. Next, an appropriate amount of G, AC, or CSCNT-AC was added to the same volume of the microemulsion prepared above, and the mixture was stirred at room temperature for 1 h in the case of G and AC. As for CSCNT-AC, the mixture was stirred at room temperature for 24 h to increase the efficiency of Pd incorporation into CSCNT-AC. The resulting Pd catalysts (Pd/G, Pd/AC, and Pd/CSCNT-AC) were filtered through 0.22-μm PVDF membranes (Merck-Millipore), rinsed thoroughly with ethanol, and dried at 100 °C for 24 h. Several catalysts were prepared by depositing different Pd concentrations over the three types of supports, to afford Pd/G (0.7 and 2.2 wt%), Pd/AC (1.0 and 1.7 wt%), and Pd/CSCNT-AC (0.9 and 2.0 wt%). The specific surface areas of Pd/G, Pd/AC, and Pd/CSCNT-AC, determined from BET $N_2$ isotherms, were 95, 210, and 148 $m^2\ g^{-1}$, respectively.

### 3.4 Procedure for 5-hydroxymethylfurfural (HMF) hydrogenation

HMF hydrogenation reactions were carried out in a 150-mL stainless steel reactor under magnetic stirring. The reaction temperature was controlled with a thermostatic silicone oil bath. 50 mg of HMF (0.40 mmol) and 5 mg of the catalyst (Pd/G, Pd/AC, or Pd/CSCNT-AC) were suspended in 6 mL of deionized water [37]. The vessel was purged with hydrogen three times and pressurized with hydrogen at the desired pressure. The reaction mixture was stirred under certain experimental conditions for the desired time. After the

reaction was complete, the reactor was rapidly cooled below room temperature in cold water bath and depressurized. The reaction mixture was filtered through filter paper, to remove the catalyst. The aqueous phase obtained after filtration was extracted with ethyl acetate (3 x 5 mL). The organic phase was dried over anhydrous magnesium sulfate and analyzed by gas chromatography to determine the starting material conversion rate and the product ratio. Then, the solvent was evaporated, and the residue was analyzed by FTIR, $^{1}H$ and $^{13}C$ NMR, and mass spectroscopy to confirm the product structures.

## 4. Conclusions

Selectivity toward BHMF formation and HMF conversion reveals the importance of having Pd incorporated into a substrate that contains hydrophobic and hydrophilic regions. Pd incorporated into hydrophobic G provides better results than Pd incorporated into hydrophilic AC. In turn, the Pd/CSCNT-AC composite arises as the catalyst with the best performance, which is enhanced with increasing temperature, while its selectivity toward BHMF remains unaltered. Regarding the hydrogen pressure effect on HMF hydrogenation, HMF conversion increases with pressure for all kinds of catalysts, as expected, whilst selectivity toward BHMF decreases a lot, mainly in the case of the catalyst prepared with Pd adsorbed onto hydrophobic or hydrophilic substrates (G or AC). With increasing pressure, hydrogen can adsorb onto the carbonaceous material surface, which in turn can affect Pd adsorption. When Pd is not in contact with the substrate, it acts on HMF conversion but decreases reaction selectivity.

In summary, we have demonstrated that the excellent performance of Pd/CSCNT-AC toward selective BHMF production is due to the hybrid hydrophobic/hydrophilic architecture of the support, which can aid the role of water in the studied reactions and increase the selectivity toward carbonyl group hydrogenation. However, the interesting behavior of CSCNTs with respect to water molecules can also influence the results, which means that CNTs with another structure can lead to a different result.

## Acknowledgments

The authors thank FAPESP (grants # 2017/04759-2, and 2018/24680-4), CNPq (grant 311647/2021-9), and CAPES for financial support and fellowships. The authors thank Center for Nanotechnology Applied to the Chemical Industry (CNAI) of the DQ-FFCLRP-USP, the Brazilian Nanotechnology National Laboratory, LNNano/CNPEM, Campinas, SP, Brazil; and the Physics Division of the University of Camerino, Italy, for the characterization of catalysts. The authors also thank Cynthia M. C. P. Manso for reviewing the text.

## Author Contributions

Wesley R. Silva: Investigation, Writing - original draft; José M. Rosolen: Supervision, Writing - review & editing; Paulo M. Donate: Conceptualization, Supervision, Writing - review & editing.

## References and Notes

[1] Chidambaram, M.; Bell, A. T. *Green Chem*. **2010**, *12*, 1253. [Crossref]

[2] Román-Leshkov, Y.; Chheda, J. N.; Dumesic, J. A. *Science* **2006**, *312*, 1933. [Crossref]

[3] Zu, Y.; Yang, P.; Wang, J.; Liu, X.; Ren, J.; Lu, G.; Wang, Y. *Appl. Catal. B: Environ*. **2014**, *146*, 244. [Crossref]

[4] Fang, Z.; Smith Jr., R. L.; Qi, X., eds. Production of Platform Chemicals from Sustainable Resources, Heidelberg Berlin: Springer-Verlag, 2017.

[5] Alamillo, R.; Tucker, M.; Chia, M.; Pagán-Torres, Y.; Dumesic, J. *Green Chem*. **2012**, *14*, 1413. [Crossref]

[6] Galaverna, R.; Breitkreitz, M. C.; Pastre, J. C. *ACS Sust. Chem. Eng*. **2018**, *6*, 4220. [Crossref]

[7] Phan, H. B.; Nguyen, Q. B. T.; Luong, C. M.; Tran, K. N.; Tran, P. H. *Mol. Cat.* **2021**, *503*, 111428. [Crossref]

[8] Rosatella, A. A.; Simeonov, S. P.; Frade, R. F. M.; Afonso, C. A. M. *Green Chem*. **2011**, *13*, 754. [Crossref]

[9] Hou, Q.; Qi, X.; Zhen, M.; Qian, H.; Nie, Y.; Bai, C.; Zhang, S.; Bai, X.; Ju, M. *Green Chem*. **2021**, *23*, 119. [Crossref]

[10] Nishimura, S.; Ikeda, N.; Ebitani, K. *Catal. Today* **2014**, *232*, 89. [Crossref]

[11] Delidovich, I.; Hausoul, P. J. C.; Deng, L.; Pfutzenreuter, R.; Rose, M.; Palkovits, R. *Chem. Rev*. **2016**, *116*, 1540. [Crossref]

[12] Fulignati, S.; Antonetti, C.; Licursi, D.; Pieraccioni, M.; Wilbers, E.; Heeres, H. J.; Galletti, A. M. R. *Applied Catal. A, General* **2019**, *578*, 122. [Crossref]

[13] Fulignati, S.; Antonetti, C.; Wilbers, E.; Licursi, D.; Heeres, H. J.; Galletti, A. M. R. *J. Ind. Eng. Chem.* **2021**, *100*, 390.e1. [Crossref]

[14] Mitra, J.; Zhou, X.; Rauchfuss, T. *Green Chem*. **2015**, *17*, 307. [Crossref]

[15] Kitanosono, T.; Masuda, K.; Xu, P.; Kobayashi, S. *Chem. Rev*. **2018**, *118*, 679. [Crossref]

[16] Tang, X.; Wei, J.; Ding, N.; Sun, Y.; Zeng, X.; Hu, L.; Liu, S.; Lei, T.; Lin, L. *Renew. Sust. Energy Rev*. **2017**, *77*, 287. [Crossref]

[17] Upare, P. P.; Hwang, Y. K.; Hwang, D. W. *Green Chem*. **2018**, *20*, 879. [Crossref]

[18] Gupta, K.; Rai, R. K.; Singh, S. K. *ChemCatChem*, **2018**, *10*, 2326. [Crossref]

[19] Wang, Q.; Feng, J.; Zheng, L.; Wang, B.; Bi, R.; He, Y.; Liu, H.; Li, D. *ACS Catal*. **2020**, *10*, 1353. [Crossref]

[20] Chen, S.; Wojcieszak, R.; Dumeignil, F.; Marceau, E.; Royer, S. *Chem. Rev*. **2018**, *118*, 11023. [Crossref]

[21] Wiesfeld, J. J.; Kim, M.; Nakajima, K.; Hensen, E. J. M. *Green Chem*. **2020**, *22*, 1229. [Crossref]

[22] Wang, T.; Wei, J.; Liu, H.; Feng, Y.; Tang, X.; Zeng, X.; Sun, Y.; Lei, T.; Lin, L. *J. Ind. Eng. Chem.* **2020**, *81*, 93. [Crossref]

[23] Ma, N.; Song, Y.; Han, F.; Waterhouse, G. I. N.; Li, Y.; Ai, S. *Catal. Sci. Technol.* **2020**, *10*, 4010. [Crossref]

[24] Chatterjee, M.; Ishizaka, T.; Kawanami, H. *Green Chem*., **2014**, *16*, 1543. [Crossref]

[25] Kozbial, A.; Zhou, F.; Li, Z.; Liu, H.; Li, L. *Acc. Chem. Res*. **2016**, *49*, 2765. [Crossref]

[26] Goto, T.; Amano, Y.; Machida, M.; Imazeki, F. *Chem. Pharm. Bull.* **2015**, *63*, 726. [Crossref]

[27] Matsubara, E. Y.; Takahashi, G. H.; Macedo, N. G.; Gunnella, R.; Rosolen, J. M. *J. Electroanal. Chem*. **2016**, *765*, 58. [Crossref]

[28] Rosolen, J. M.; Matsubara, E. Y.; Marchesin, M. S.; Lala,

S. M.; Montoro, L. A.; Tronto, S. *J. Power Sources* **2006**, *162*, 620. [Crossref]

[29] Moraes, I. R.; Matsubara, E. Y.; Rosolen, J. M. *Electrochem. Solid State Lett*. **2008**, *11*, K109. [Crossref]

[30] Freitas Neto, D. B.; Xavier, F. F. S.; Matsubara, E. Y.; Parmar, R.; Gunnella, R.; Rosolen, J. M. *J. Electroanal. Chem*. **2020**, *858*, 113826. [Crossref]

[31] Endo, M.; Kim, Y. A.; Hayashi, T.; Fukai, Y.; Oshida, K.; Terrones, M.; Yanagisawa, T.; Higaki, S.; Dresselhaus, M. S. *Appl. Phys. Lett*. **2002**, *80*, 1267. [Crossref]

[32] Li, Q. Y.; Matsushita, R.; Tomo, Y.; Ikuta, T.; Takahashi, K. *J. Phys. Chem. Lett*. **2019**, *10*, 3744. [Crossref]

[33] Liu, S.; Amada, Y.; Tamura, M.; Nakagawa, Y.; Tomishige, K. *Green Chem*. **2014**, *16*, 617. [Crossref]

[34] Nascimento, L. F.; Matsubara, E. Y.; Donate, P. M.; Rosolen, J. M. *Reac. Kinet. Mech. Catal*. **2013**, *110*, 471. [Crossref]

[35] Ribeiro, P. H. Z.; Matsubara, E. Y.; Rosolen, J. M.; Donate, P. M.; Gunnella, R. *J. Mol. Catal. A: Chem*. **2015**, *410*, 34. [Crossref]

[36] Souza Filho, J.; Matsubara, E. Y.; Franchi, L. P.; Martins, I. P.; Rivera, L. M. R.; Rosolen, J. M.; Grisolia, C. K. *Environ. Res*. **2014**, *134*, 9. [Crossref]

[37] Silva, W. R.; Matsubara, E. Y.; Rosolen, J. M.; Donate, P. M.; Gunnella, R. *Mol. Catal.* **2021**, *504*, 111496. [Crossref]

[38] Cao, Y.; Chen, Z. X. *Surf. Sci*. **2006**, *600*, 4572. [Crossref]

[39] Silva, W. R. Preparation and applications of heterogeneous catalysts supported in nanostructured composites of carbon. [Master's thesis.] Ribeirão Preto, SP, Brazil: Universidade de São Paulo, 2017. [Crossref]

## How to cite this article

Da Silva, W. R.; Rosolen, J. M.; Donate, P. M. *Orbital: Electron. J. Chem.* **2022**, *14*, 74. DOI: http://dx.doi.org/10.17807/orbital.v14i2.15596